ISSN 0021-8944, Journal of Applied Mechanics and Technical Physics, 2017, Vol. 58, No. 2, pp. 291–300. © Pleiades Publishing, Ltd., 2017.
Original Russian Text © A. Ghafouri, N. Pourmahmoud, and A. F. Jozaei.

NUMERICAL SIMULATION OF THE NANOPARTICLE DIAMETER EFFECT ON THE THERMAL PERFORMANCE OF A NANOFLUID IN A COOLING CHAMBER

A. Ghafouri[a], N. Pourmahmoud[b], and A. F. Jozaei[a]

UDC 536.2

Abstract: The thermal performance of a nanofluid in a cooling chamber with variations of the nanoparticle diameter is numerically investigated. The chamber is filled with water and nanoparticles of alumina (Al_2O_3). Appropriate nanofluid models are used to approximate the nanofluid thermal conductivity and dynamic viscosity by incorporating the effects of the nanoparticle concentration, Brownian motion, temperature, nanoparticles diameter, and interfacial layer thickness. The horizontal boundaries of the square domain are assumed to be insulated, and the vertical boundaries are considered to be isothermal. The governing stream-vorticity equations are solved by using a second-order central finite difference scheme coupled with the mass and energy conservation equations. The results of the present work are found to be in good agreement with the previously published data for special cases. This study is conducted for the Reynolds number being fixed at Re = 100 and different values of the nanoparticle volume fraction, Richardson number, nanofluid temperature, and nanoparticle diameter. The results show that the heat transfer rate and the Nusselt number are enhanced by increasing the nanoparticle volume fraction and decreasing the Richardson number. The Nusselt number also increases as the nanoparticle diameter decreases.

Keywords: nanofluid, nanoparticle diameter, heat transfer enhancement, Nusselt number.

DOI: 10.1134/S0021894417020134

INTRODUCTION

The cooling or heating performance of thermal systems (nuclear reactors or solar arrays) plays a vital role in the development of energy-efficient heat transfer equipment. It was shown [1] that the thermal conductivity of a nanofluid is much higher than that of a base fluid even if the nanoparticle volume fraction in the mixture is rather low. Various engineering applications of nanofluids were discussed in [2–5].

As the flow and thermal behavior of nanofluids are very sophisticated, several theoretical and experimental models have been developed to estimate the thermophysical properties of nanofluids. These models are based on the temperature, Brownian motion, nanoparticle diameter and shape, and interfacial layer thickness [6–8]. Mixed convection as well as natural convection heat transfer and nanofluid flow in a two-dimensional cooling chamber have been extensively investigated [9–13].

What is common in most of the above-referenced work is the use of traditional viscosity and thermal conductivity models for a nanofluid, which predict the main reason for heat transfer enhancement to be the presence of nanoparticles, regardless of the nanoparticle diameter.

[a]Department of Mechanical Engineering, Ahvaz Branch, Islamic Azad University, Ahvaz, Iran; a.ghafouri@iauahvaz.ac.ir, falavand@iauahvaz.ac.ir. [b]Department of Mechanical Engineering, Urmia University, Urmia, Iran; n.pormahmod@urmia.ac.ir. Translated from Prikladnaya Mekhanika i Tekhnicheskaya Fizika, Vol. 58, No. 2, pp. 122–132, March–April, 2017. Original article submitted September 18, 2015.

Murshed et al. [14] focused on various investigations of nanofluids, such as analytical and experimental studies on the effective thermal conductivity and convective heat transfer. They deduced that the existing classical models cannot predict the viscosity and effective thermal diffusivity of nanofluids. Pourmahmoud et al. [15] numerically studied laminar mixed convection in a lid-driven square cavity filled with a nanofluid by using eight different nanofluid viscosity models. They found that the heat transfer rate is moderately accentuated by reducing the Richardson number and increasing the nanoparticle volume fraction. They indicated that a proper choice of the viscosity model is one of the main factors that helps to ensure a correct prediction of the heat transfer rate and Nusselt number. In addition, older models, such as the Brinkman viscosity model [16] and the Maxwell thermal conductivity model [17], cannot predict the nanofluid properties as functions of the temperature, Brownian motion, and nanoparticle diameter.

The effects of the nanoparticle diameter and temperature on the heat transfer rate in a nanofluid were taken into account in thermal conductivity models [18–21] and dynamic viscosity models [22–25].

Hwang et al. [26] theoretically investigated the thermal characteristics of natural convection in a rectangular cavity containing a water-based nanofluid heated from below. They showed that the heat transfer coefficient decreases with increasing nanoparticle diameter and decreasing temperature. Lin and Violi [27] numerically investigated the effects of the particle diameter and temperature on natural convection heat transfer of an alumina–water nanofluid in a vertical cavity. They also studied the heat transfer rate in a nanofluid containing particles of different diameters as a function of the mean diameter of nanoparticles, their volume fraction in the nanofluid, and Prandtl and Grashof numbers. They deduced that the heat transfer characteristics can be enhanced by decreasing the nanoparticle diameter from 250 to 5 mm.

The presented work is aimed at studying mixed convection flows of the alumina–water nanofluid in a square cooling chamber whose walls move uniformly in the horizontal plane. The left vertical wall has a higher temperature than the right vertical wall. Both the top and bottom walls are insulated. The effective thermal conductivity of the nanofluid is calculated as a function of the nanoparticle diameter by using the model proposed by Chon et al. [20]. The model developed by Masoumi et al. [23] is used to determine the nanofluid viscosity. The consequences of varying the nanoparticle diameter, nanoparticle volume fraction, bulk temperature, and Richardson number on the hydrodynamic and thermal characteristics are investigated and discussed.

1. PHYSICAL CONFIGURATION AND GOVERNING EQUATIONS

Figure 1 shows a schematic diagram of a two-dimensional cooling chamber filled with a suspension of alumina nanoparticles in water. The top wall is moving rightward with a uniform velocity U_m. The left wall is heated and maintained at a constant temperature T_h higher than the temperature of the right wall T_c ($T_h > T_c$), whereas the top and bottom horizontal walls are thermally insulated. The nanofluid in the chamber is considered to be Newtonian, and the flow is laminar.

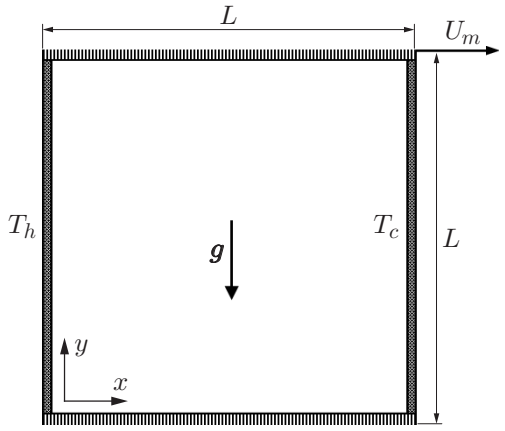

Fig. 1. Geometry of the present study.

The dimensionless governing equations in the Cartesian coordinate system for the stream function Ψ, vorticity function Ω, and thermal transport θ can be written as

$$\frac{\partial^2\Psi}{\partial X^2}+\frac{\partial^2\Psi}{\partial Y^2}=-\Omega,$$

$$U\frac{\partial\Omega}{\partial X}+V\frac{\partial\Omega}{\partial Y}=\frac{\mu_{nf}/\mu_f}{1-\varphi+\varphi\rho_{np}/\rho_f}\frac{1}{\mathrm{Re}}\Big(\frac{\partial^2\Omega}{\partial X^2}+\frac{\partial^2\Omega}{\partial Y^2}\Big)+\Big(1-\varphi+\varphi\frac{\beta_{np}}{\beta_f}\Big)\frac{\mathrm{Ra}}{\mathrm{Pr}\ \mathrm{Re}^2}\frac{\partial\theta}{\partial X}, \tag{1}$$

$$U\frac{\partial\theta}{\partial X}+V\frac{\partial\theta}{\partial Y}=\frac{k_{nf}/k_f}{1-\varphi+\varphi\,(\rho c_p)_{np}/(\rho c_p)_f}\frac{1}{\mathrm{Re}\,\mathrm{Pr}}\Big(\frac{\partial^2\theta}{\partial X^2}+\frac{\partial^2\theta}{\partial Y^2}\Big),$$

where the Reynolds number Re, the Prandtl number Pr , the Rayleigh number Ra, and the Richardson number Ri are defined as

$$\mathrm{Re}=\frac{U_mL}{\nu_f},\qquad \mathrm{Pr}=\frac{\nu_f}{\alpha_f},\qquad \mathrm{Ra}=\frac{g\beta_f(T_h-T_c)L^3}{\alpha_f\nu_f},\qquad \mathrm{Ri}=\frac{\mathrm{Ra}}{\mathrm{Pr}\ \mathrm{Re}^2},$$

Ψ, Ω, U, and V are additional dimensionless variables:

$$\Psi=\frac{\psi}{U_mL},\qquad \Omega=\frac{\omega L}{U_m},\qquad U=\frac{\partial\Psi}{\partial Y},\qquad V=-\frac{\partial\Psi}{\partial X}.$$

The dimensionless boundary conditions used to solve Eqs. (1) are

$$U=V=\Psi=0,\qquad \theta=1,\qquad \Omega=-\frac{\partial^2\Psi}{\partial X^2} \tag{2}$$

on the left wall,

$$U=V=\Psi=0,\qquad \theta=0,\qquad \Omega=-\frac{\partial^2\Psi}{\partial X^2} \tag{3}$$

on the right wall,

$$V=\Psi=0,\qquad U=1,\qquad \frac{\partial\theta}{\partial Y}=0,\qquad \Omega=-\frac{\partial^2\Psi}{\partial Y^2} \tag{4}$$

on the top wall, and

$$V=\Psi=0,\qquad U=-1,\qquad \frac{\partial\theta}{\partial Y}=0,\qquad \Omega=-\frac{\partial^2\Psi}{\partial Y^2} \tag{5}$$

on the bottom wall.

2. THERMOPHYSICAL PROPERTIES AND NANOFLUID MODELS

The thermophysical properties of pure water and Al_2O_3 nanoparticles at a temperature of 25°C are listed in Table 1 [28]. All thermophysical properties are assumed to be constant, except for density, which is approximated by the Boussinesq model.

The effective density ρ_{nf}, heat capacitance $(\rho c_p)_{nf}$, thermal diffusivity α_{nf}, and thermal expansion coefficient $(\rho\beta)_{nf}$ of the nanofluid are defined as follows [29]:

$$\rho_{nf}=(1-\varphi)\rho_f+\varphi\rho_{np},\qquad (\rho c_p)_{nf}=(1-\varphi)(\rho c_p)_f+\varphi(\rho c_p)_{np},$$

$$\alpha_{nf}=k_{nf}/(\rho c_p)_{nf},\qquad (\rho\beta)_{nf}=(1-\varphi)(\rho\beta)_f+\varphi(\rho\beta)_{np}.$$

Table 1. Thermophysical properties of the fluid and nanoparticles [28]

Nanofluid component	c_p, J/(kg · K)	ρ, kg/m^3	k, W/(m · K)	$\beta\cdot10^{-5}$, K^{-1}
Water	4179	997.1	0.613	21.00
Al_2O_3 nanoparticles	765	3970.0	25.000	0.85

The effective viscosity of the nanofluid as a function of the temperature, Brownian motion, and nanoparticle diameter is approximated in accordance with the model proposed by the Masoumi et al. [23]:

$$\frac{\mu_{nf}}{\mu_f} = 1 + \frac{\rho_{np} V_B d_{np}^2}{72 C \delta \mu_f}.$$

Here the Brownian motion velocity V_B, the distance between the nanoparticles δ, and the correction factor C are defined as

$$V_B = \frac{1}{d_{np}} \sqrt{\frac{18 k_B T}{\pi \rho_{np} d_{np}}}, \qquad \delta = \sqrt[3]{\frac{\pi}{6\varphi}}\, d_{np},$$

$$C = 10^{-5}(-(0.1133 d_{np} + 0.2771)\varphi + 0.009 d_{np} - 0.0393)/\mu_f.$$

The model of Masoumi et al. [23] describes nanofluids consisting of alumina, titanium, and copper oxide nanoparticles suspended in water or ethylene glycol with the nanoparticle volume fraction varying in the range $\varphi = 0.01$–0.05 at temperatures in the interval $T = 293$–340 K [23]. The results of this model are in good agreement with the experimental data of Nguyen et al. [30].

In order to model the thermal conductivity of the nanofluid, Chon el al. [20] derived the relation

$$\frac{k_{nf}}{k_f} = 1 + 64.7 \varphi^{0.7640} \Big(\frac{d_f}{d_{np}}\Big)^{0.3690} \Big(\frac{k_{np}}{k_f}\Big)^{0.7476} \mathrm{Pr}_T^{0.9955}\, \mathrm{Re}_T^{1.2321},$$

where

$$\mathrm{Pr}_T = \frac{\mu_f}{\rho_f \alpha_f}, \qquad \mathrm{Re}_T = \frac{\rho_f k_\mathrm{B} T}{3\pi \mu_f^2 l_f}, \qquad l_f = \frac{1}{\sqrt{2m}\, \pi d_f^2},$$

$k_\mathrm{B} = 1.3807 \cdot 10^{-23}$ J/K is the Boltzmann constant, and $l_f = 0.17$ nm is the mean free path of the base fluid particles [20].

The model [20] includes the effect of the nanoparticle diameter and temperature on the thermal conductivity of the nanofluid in a wide range of temperatures $T = 21$–$70°$C. The accuracy of this model was confirmed by the experiments of Minsta et al. [31].

3. NUMERICAL METHOD AND CODE VALIDATION

Equations (1) with the boundary conditions (2)–(5) are solved by using the second-order central difference scheme. The successive overrelaxation method is used to solve the stream function equation.

Numerical implementation of the algorithm for solving the stream function, vorticity, and temperature equations and the procedure of advancement to a next time is performed in the FORTRAN programming language. The steady state solution is assumed to be reached when the tolerance λ between two successive time steps ($d\tau = 0.0017$) is smaller than 10^{-6}. The convergence criterion is defined by the expression

$$\lambda = \sum_{j=1}^{j=M} \sum_{i=1}^{i=N} |\gamma^{n+1} - \gamma^n| \;\Big/\; \sum_{j=1}^{j=M} \sum_{i=1}^{i=N} |\gamma^{n+1}| \leqslant 10^{-6},$$

where M and N are the numbers of grid points in the X and Y direction, respectively. The symbol γ denotes any scalar transport quantity: Ψ, Ω, or θ.

The local and average heat transfer rates in the chamber can be presented by means of the local and average Nusselt numbers. The local Nusselt number Nu is calculated on the left heated wall, and the average Nusselt number Nu_{av} is determined by integrating the local Nusselt number along the heated wall:

$$\mathrm{Nu}(Y) = \frac{k_{nf}}{k_f} \frac{\partial \theta}{\partial X}\Big|_{X=0};$$

$$\mathrm{Nu}_{av} = \int_0^1 \mathrm{Nu}\,(X)\, dY. \tag{6}$$

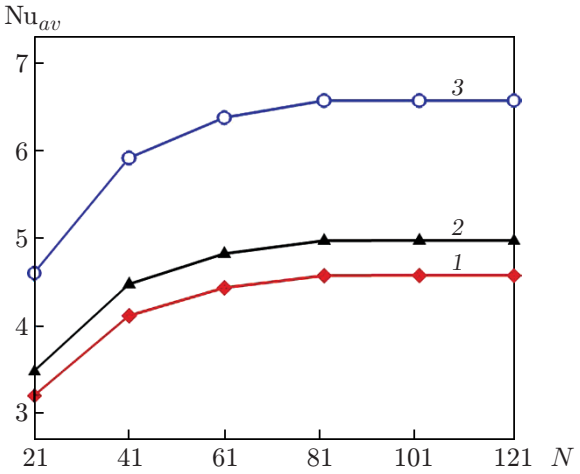

Fig. 2. Averaged Nusselt number versus the computational grid size N for different Rayleigh numbers: $\mathrm{Ra} = 1.75 \cdot 10^3$ (*1*), $1.75 \cdot 10^4$ (*2*), and $1.75 \cdot 10^5$ (*3*).

Table 2. Average Nusselt number on the hot wall for different Rayleigh numbers

Reference	Nu_{av}			
	$\mathrm{Ra} = 10^3$	$\mathrm{Ra} = 10^4$	$\mathrm{Ra} = 10^5$	$\mathrm{Ra} = 10^6$
Present work	1.123	2.246	4.521	8.984
[35]	1.120	2.242	4.514	8.790
[29]	1.118	2.245	4.522	8.826
[34]	1.052	2.302	4.646	9.012
[33]	1.108	2.201	4.430	8.754
[32]	1.118	2.243	4.519	8.79

For convenience, a normalized average Nusselt number Nu^*_{av} is defined as the ratio of the Nusselt number at a certain volume fraction of nanoparticles φ to that of pure water [28]:

$$\mathrm{Nu}^*_{av}(\varphi) = \frac{\mathrm{Nu}_{av}(\varphi)}{\mathrm{Nu}_{av}\big|_{\varphi=0}}.$$

The present code was tested for grid independence by calculating the average Nusselt number on the left wall for different Rayleigh numbers on 21×21, 41×41, 61×61, 81×81, 101×101, and 121×121 computational grids (Fig. 2). It is seen that an 81×81 uniform grid is sufficiently fine to ensure a grid-independent solution. Further grid refinement does not alter the results of computations. In addition, the governing equations were solved for the natural convection flow in a cavity filled with pure water in order to compare the results with those obtained previously [29, 32–35] (Table 2).

4. RESULTS AND DISCUSSION

The effects of the nanoparticle diameter on the thermal performance of the nanofluid (water containing alumina particles) in the cooling chamber are numerically studied and reported below. We calculated the local and average Nusselt numbers on the hot wall of the chamber for the Richardson numbers Ri = 0.1, 1.0, and 10.0 in the temperature range $T = 25$–65°C for the nanoparticle volume fractions $\varphi = 0.01$, 0.02, 0.03, and 0.04. Three nanoparticle diameters are used: $d_{np} = 30$, 60, and 90 nm. The calculated results are shown in Figs. 3–8.

Figure 3 depicts the variation of the average Nusselt number and normalized average Nusselt number as functions of the nanoparticle volume fraction. It is seen from Fig. 3a that the average Nusselt number at $T = 25^\circ$C increases with increasing nanoparticle volume fraction and decreases with increasing nanoparticle diameter. As the

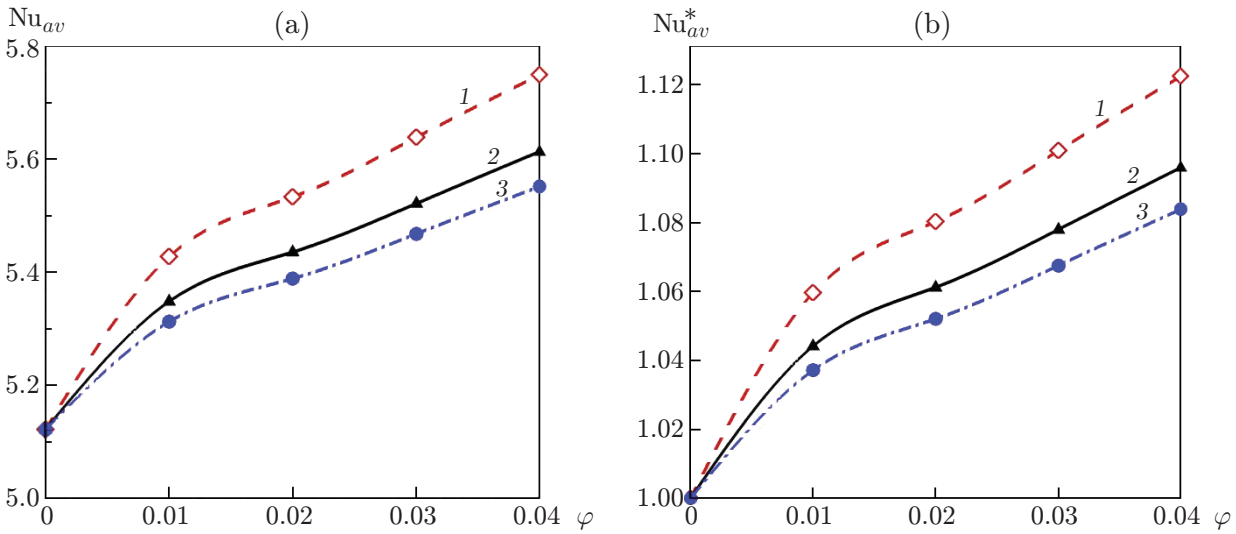

Fig. 3. Average (a) and normalized average (b) Nusselt numbers versus the nanoparticle volume fraction for Ri = 1, $T = 25°$C, and $d_{np} = 30$ (*1*), 60 (*2*), and 90 nm (*3*).

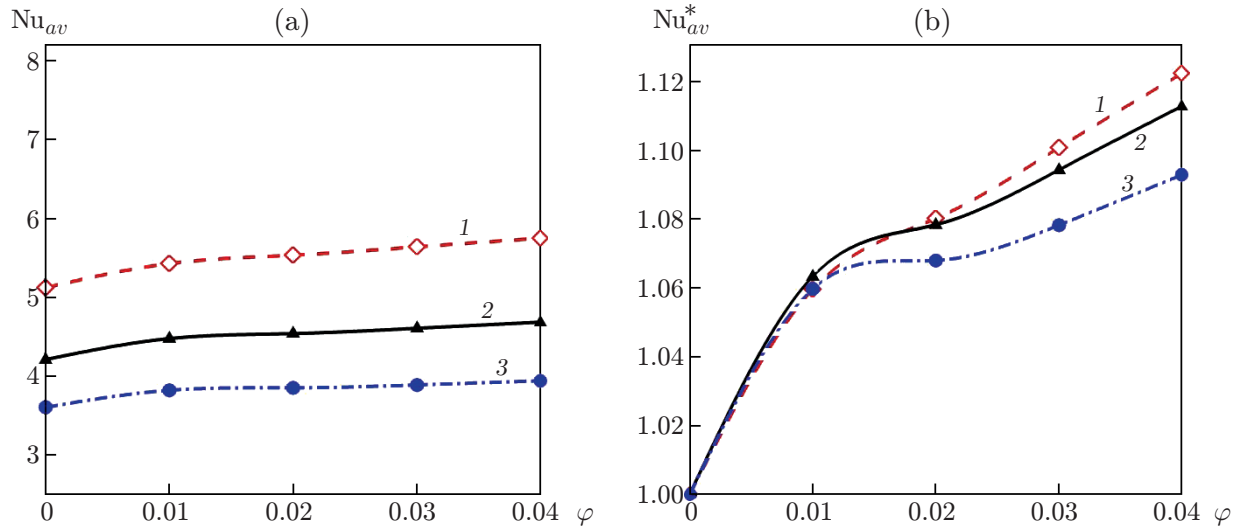

Fig. 4. Averaged (a) and normalized average (b) Nusselt numbers versus the nanoparticle volume fraction for Ri = 1, $d_{np} = 30$ nm, and $T = 25$ (*1*), 45 (*2*), and 65°C (*3*).

nanoparticle volume fraction φ increases from 0 to 0.04 at the Richardson number Ri = 1 corresponding to the mixed convection mode, the average Nusselt number increases by 12% at $d_{np} = 30$ nm and by 8% at $d_{np} = 90$ nm (see Fig. 3b). The highest average Nusselt number $\mathrm{Nu}_{av} = 5.75$ is observed at the smallest nanoparticle diameter $d_{np} = 30$ nm, as predicted by the thermal conductivity model of Chon et al. [20], which takes into account the role of the Brownian motion, nanofluid temperature, and nanoparticle diameter (see Fig. 3b).

Figure 4 presents the average and normalized average Nusselt numbers as functions of the nanoparticle volume fraction for $d_{np} = 30$ nm and different nanofluid bulk temperatures. It is seen that there is always considerable enhancement of heat transfer owing to a decrease in the bulk temperature from 65 to 25°C, regardless of the nanoparticle volume fraction. At higher temperatures, the Prandtl number decreases; hence, the heat transfer rate and the average Nusselt number also decrease. Nevertheless, a 4% increase in the volume fraction of alumina nanoparticles leads to an increase in the Nusselt number on the hot wall approximately by 9%.

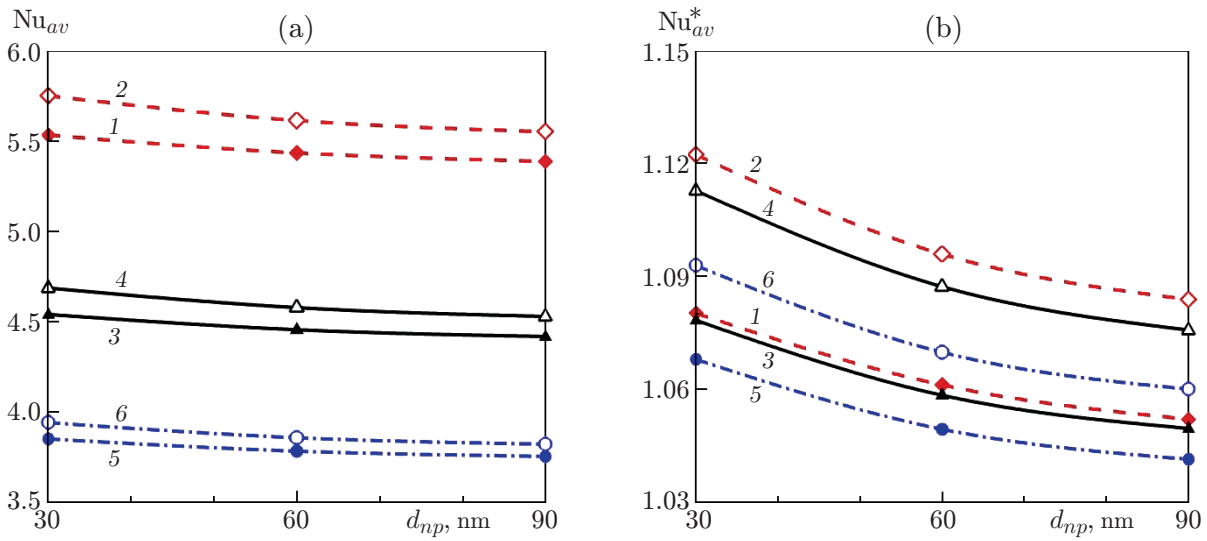

Fig. 5. Average (a) and normalized average (b) Nusselt number versus the nanoparticle diameter for Ri = 1 and different values of the nanoparticle volume fraction and nanofluid temperature: $\varphi = 0.02$ (*1*, *3*, and *5*) and 0.04 (*2*, *4*, and *6*); $T = 25$ (*1* and *2*), 45 (*3* and *4*), and 65°C (*5* and *6*).

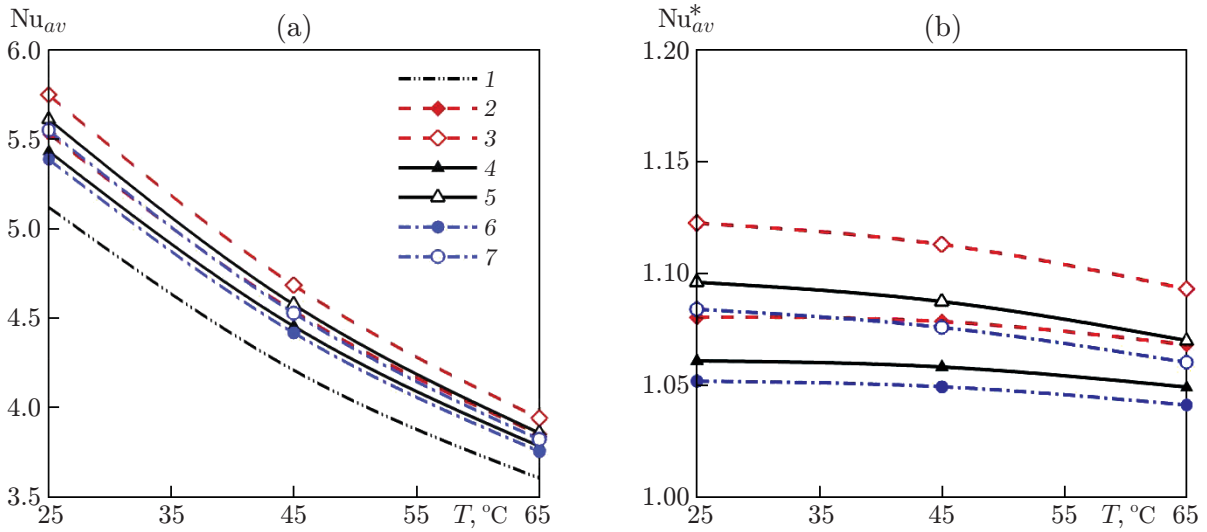

Fig. 6. Average (a) and normalized average (b) Nusselt numbers versus the nanofluid temperature for Ri = 1 and different values of the nanoparticle diameter and nanoparticle volume fraction: (*1*) pure base fluid; (*2*–*7*) nanofluid; $d_{np} = 30$ (*2* and *3*), 60 (*4* and *5*), and 90 nm (*6* and *7*); $\varphi = 0.02$ (*2*, *4*, and *6*) and 0.04 (*3*, *5*, and *7*).

Figure 5 illustrates the effect of the nanoparticle diameter on the average and normalized average Nusselt numbers for different temperatures and nanoparticle volume fractions. It is clear that an increase in the nanoparticle diameter leads to reduction of the heat transfer rate on the hot wall of the cooling chamber.

The same trend is shown in Fig. 6: the heat transfer rate on the hot wall of the cooling chamber decreases with increasing nanofluid bulk temperature, regardless of the nanoparticle volume fraction and nanoparticle diameter.

Figures 7 and 8 demonstrate the effect of the Richardson number on the average Nusselt number for different values of the nanoparticle diameter and nanofluid bulk temperature. It is seen that the average Nusselt number decreases as the Richardson number increases from 0.1 to 10.0.

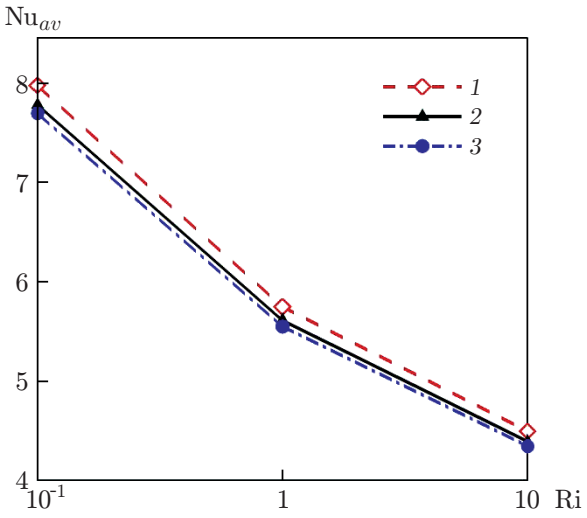

Fig. 7.

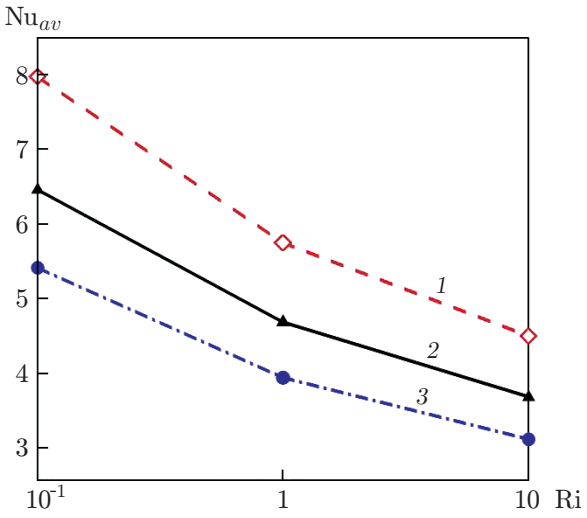

Fig. 8.

Fig. 7. Average Nusselt number versus the Richardson number for $T = 25°C$ and $d_{np} = 30$ (*1*), 60 (*2*), and 90 nm (*3*).

Fig. 8. Average Nusselt number versus the Richardson number for $d_{np} = 30$ nm and $T = 25$ (*1*), 45 (*2*), and 65°C (*3*).

At $\varphi = 0.04$, $T = 25°C$, and Ri = 0.1, 1.0, and 10.0, the average Nusselt numbers on the hot wall for the nanofluid containing nanoparticles with a diameter of 30 nm are $\mathrm{Nu}_{av} = 7.9$, 5.7, and 4.5, respectively (see Fig. 7). For the nanofluid bulk temperature $T = 65°C$ and Ri = 0.1, 1.0, and 10.0, the average Nusselt numbers on the hot wall are $\mathrm{Nu}_{av} = 5.4$, 3.9, and 3.1, respectively (see Fig. 8).

CONCLUSIONS

A mixed convection heat transfer problem for a nanofluid flow (water containing alumina particles) in a cooling chamber is studied for different Richardson numbers and different nanoparticle volume fractions.

Appropriate nanofluid models are used to approximate the nanofluid thermal conductivity and nanofluid dynamic viscosity, which incorporate the effects of the nanoparticle volume fraction, Brownian motion, temperature, nanoparticle diameter, and interfacial layer thickness on the heat transfer characteristics.

The main findings can be summarized as follows. The Nusselt number and heat transfer rate from the left wall of the cooling chamber are enhanced by increasing the nanoparticle volume fraction. The heat transfer rate increases with decreasing Richardson number and other parameters of the process being fixed, regardless of the nanoparticle diameter and nanofluid bulk temperature. The heat transfer characteristics of the nanofluid can be enhanced by increasing the nanoparticle diameter from 30 to 90 nm. It is recognized that the normalized average Nusselt number appreciably depends on the nanoparticle diameter at high nanoparticle volume fractions. As the bulk temperature decreases from 65 to 25°C, the normalized average Nusselt number increases, regardless of the nanoparticle diameter.

REFERENCES

1. S. U. S. Choi, "Enhancing Thermal Conductivity of Fluids with Nanoparticles," ASME Fluids Eng. Div. **231**, 99–105 (1995).
2. V. Trisaksri and S. Wongwises, "Critical Review of Heat Transfer Characteristics of Nanofluids," Renewable Sustainable Energy Rev. **11**, 512–523 (2007).

3. W. Daungthongsuk and S. Wongwises, "A Critical Review of Convective Heat Transfer Nanofluids," Renewable Sustainable Energy Rev. **11**, 797–817 (2007).
4. S. Kakac and A. Pramuanjaroenkij, "Review of Convective Heat Transfer Enhancement with Nanofluids," Int. J. Heat Mass Transfer **52**, 3187–3196 (2009).
5. R. Saidur, K. Y. Leong, and H. A. Mohammad, "A Review on Applications and Challenges of Nanofluids," Renewable Sustainable Energy Rev. **15**, 1646–1668 (2011).
6. J. Buongiorno, D. C. Venerus, N. Prabhat, et al., "A Benchmark Study on the Thermal Conductivity of Nanofluids," J. Appl. Phys. **106** (9), 094312 (2009).
7. I. M. Mahbubul, R. Saidur, and M. A. Amalina, "Latest Developments on the Viscosity of Nanofluids," Int. J. Heat Mass Transfer **55**, 874–885 (2012).
8. W. H. Yu, D. M. France, J. L. Routbort, and S. U. S. Choi, "Review and Comparison of Nanofluid Thermal Conductivity and Heat Transfer Enhancements," Heat Transfer Eng. **29** (5), 432–460 (2008).
9. M. Muthtamilselvan, P. Kandaswamy, and J. Lee, "Heat Transfer Enhancement of Copper-Water Nanofluids in a Lid-Driven Enclosure," Comm. Nonlinear Sci. Numer. Simulat. **15**, 1501–1510 (2010).
10. G. A. Sheikhzadeh, A. Arefmanesh, M. H. Kheirkhah, and R. Abdollahi, "Natural Convection of Cu–Water Nanofluid in a Cavity with Partially Active Side Walls," Europ. J. Mech., B: Fluids **30**, 166–176 (2011).
11. C. C. Cho, H. T. Yau, and C. K. Chen, "Enhancement of Natural Convection Heat Transfer in a U-Shaped Cavity Filled with Al_2O_3–Water Nanofluid," Thermal Sci. **16** (5), 1309–1316 (2012).
12. H. F. Oztop, M. Mobedi, E. Abu-Nada, and I. Pop, "A Heatline Analysis of Natural Convection in a Square Inclined Enclosure Filled with a CuO Nanofluid under Non-Uniform Wall Heating Condition," Int. J. Heat Mass Transfer **55**, 5076–5086 (2012).
13. G. A. Sheikhzadeh, N. Hajialigol, M. Ebrahim Qomi, and A. Fattahi, "Laminar Mixed Convection of Cu–Water Nnofluid in Twosided Lid-Driven Enclosures," J. Nanostructure **1**, 44–53 (2012).
14. S. M. S. Murshed, K. C. Leang, and C. Yang, "Thermophysical and Electro Kinematic Properties of Nanofluids: A Critical Review," Appl. Thermal Eng. **28**, 2109–2125 (2008).
15. N. Pourmahmoud, A. Ghafouri, and I. Mirzaee, "Numerical Comparison of Viscosity Models on Mixed Convection in Double Lid-Driven Cavity Utilized CuO–Water Nanofluid," Thermal Sci. **20** (1), 347–358 (2016).
16. H. C. Brinkman, "The Viscosity of Concentrated Suspensions and Solutions," J. Chem. Phys. **20**, 571–581 (1952).
17. J. C. Maxwell-Garnett, "Colours in Metal Glasses and in Metallic Films," Philos. Trans. Roy. Soc. London, Ser. A **203**, 385–420 (1904).
18. J. Koo and C. Kleinstreuer, "A New Thermal Conductivity Model for Nanofluids," J. Nanoparticle Res. **6**, 577–588 (2004).
19. H. E. Patel, T. Pradeep, T. Sundararajan, et al., "A Micro-Convection Model for Thermal Conductivity of Nanofluid," Pramana J. Phys. **65**, 863–869 (2005).
20. C. H. Chon, K. D. Kihm, S. P. Lee, and S. U. S. Choi, "Empirical Correlation Finding the Role of Temperature and Particle Size for Nanofluid (Al_2O_3) Thermal Conductivity Enhancement," Appl. Phys. Lett. **87**, 153107 (2005).
21. S. S. Mallick, A. Mishra, and L. Kundan, "An Investigation into Modeling Thermal Conductivity for Alumina–Water Nanofluids," Powder Technol. **233**, 234–244 (2013).
22. J. Koo and C. Kleinstreuer, "Laminar Nanofluid Flow in Micro Heat-Sinks," Int. J. Heat Mass Transfer **48** (13), 2652–2661 (2005).
23. N. Masoumi, N. Sohrabi, and A. Behzadmehr, "A New Model for Calculating the Effective Viscosity of Nanofluids," J. Phys. D: Appl. Phys. **42** (5), 055501 (2009).
24. S. M. Hosseini, A. R.Moghadassi, and D. E. Henneke, "A New Dimensionless Group Model for Determining the Viscosity of Nanofluids," J. Thermal Anal. Calorim. **100** (3), 873–877 (2010).
25. W. H. Azmi, K. V. Sharma, R. Mamat, et al., "Correlations for Thermal Conductivity and Viscosity of Water Based Nanofluids," Materials Sci. Eng. **36** (1), 2029 (2012).
26. K. S. Hwang, J. H. Lee, and S. P. Jang, "Buoyancy-Driven Heat Transfer of Water-Based Al_2O_3 Nanofluids in a Rectangular Cavity," Int. J. Heat Mass Transfer **50**, 4003–4010 (2007).
27. K. C. Lin and A. Violi, "Natural Convection Heat Transfer of Nanofluids in a Vertical Cavity: Effects of Non-Uniform Particle Diameter and Temperature on Thermal Conductivity," Int. J. Heat Fluid Flow **31**, 236–245 (2010).

28. E. Abu-Nada, "Effects of Variable Viscosity and Thermal Conductivity of Al_2O_3–Water Nanofluid on Heat Transfer Enhancement in Natural Convection," Int. J. Heat Fluid Flow **30** (4), 679–690 (2009).
29. K. Khanafer, K. Vafai, and M. Lightstone, "Buoyancy Driven Heat Transfer Enhancement in a Two-Dimensional Enclosure Utilizing Nanofluids," Int. J. Heat Mass Transfer **46**, 3639–3653 (2003).
30. C. T. Nguyen, F. Desgranges, G. Roy, et al., "Temperature and Particle-Size Dependent Viscosity Data for Water Based Nanofluids-Hysteresis Phenomenon," Int. J. Heat Fluid Flow **28**, 1492–1506 (2007).
31. A. H. Minsta, G. Roy, C. T. Nguyen, and D. Doucet, "New Temperature and Conductivity Data for Water-Based Nanofluids," Int. J. Thermal Sci. **48** (2), 363–373 (2008).
32. G. De Vahl Davis, "Natural Convection of Air in a Square Cavity, a Benchmark Numerical Solution," Int. J. Numer. Methods Fluids **3**, 249–264 (1983).
33. N. C. Markatos and K. A. Pericleous, "Laminar and Turbulent Natural Convection in an Enclosed Cavity," Int. J. Heat Mass Transfer **27**, 772–775 (1984).
34. T. Fusegi, J. M. Hyun, K. Kuwahara, and B. Farouk, "A Numerical Study of Three Dimensional Natural Convection in a Differentially Heated Cubical Enclosure," Int. J. Heat Mass Transfer **34**, 1543–1557 (1991).
35. G. A. Sheikhzadeh, M. Ebrahim Qomi, N. Hajialigol, and A. Fattahi, "Numerical Study of Mixed Convection Flows in a Lid-Driven Enclosure Filled with Nanofluid using Variable Properties," Results Phys. **2**, 5–13 (2012).